

Multi-dimensional Effects on Photon Emission from Accretion Disks around Black Holes

Kazunori Kohri,^{1,2*} Ken Ohsuga³ and Ramesh Narayan,¹

¹*Harvard-Smithsonian Center for Astrophysics, MS-51, 60 Garden Street, Cambridge, MA 02138, USA*

²*Physics Department, Lancaster University, Lancaster, LA1 4YB, UK,*

³*Department of Physics, Rikkyo University, Toshimaku, Tokyo 171-8501, Japan*

Accepted YYYY MMM DD. Received YYYY MMM DD; in original form 2006 Nov. 29

ABSTRACT

We consider multi-dimensional effects on photon emission from accretion disks and show that these effects are especially important in supercritical accretion disks. Such disks are believed to play a role in failed supernovae and gamma-ray bursts, and possibly also in ultra-luminous X-ray sources. We show that the luminosity from a supercritical accretion disk is proportional to the logarithm of the mass accretion rate when the vertical profile of the matter density is exponential. We also give a useful analytical prescription for approximating multi-dimensional effects within a one-dimensional approach.

Key words: accretion, accretion disks — black hole physics — hydrodynamics — radiative transfer

1 INTRODUCTION

There is wide consensus that active galactic nuclei (AGNs), gamma-ray bursts (GRBs), X-ray binaries, etc., are powered by accretion flows on to compact relativistic objects, most often a black hole (BH). The best understood model of such accretion flows is the standard-disk model proposed by Shakura & Sunyaev (1973).

Recently, it has been recognized that observations of many objects cannot be explained by the standard-disk model. For instance, this model cannot produce the very high temperature ($T > 10^{10}$ K) and broad-band spectrum (extending from 10^9 to $> 10^{18}$ Hz) observed in the Galactic Center source Sgr A* and in X-ray binaries in the hard state. This has led to the idea of an advection-dominated accretion flow (ADAF, Narayan & Yi 1995, Abramowicz et al. 1995¹), which is also called a radiatively inefficient accretion flow (RIAF). The RIAF model explains the low luminosity, high temperature and optically-thin emission of these systems.²

The standard disk cannot also be applied to very high-luminosity accretion disks in which the mass-accretion rate \dot{M} exceeds the critical mass-accretion rate $\dot{M}_{\text{crit}} (\equiv L_{\text{E}}/c^2$,

where L_{E} is the Eddington luminosity). In this regime, the disk becomes optically very thick and as a result photons are partially trapped inside the accreting gas. This is the regime of interest to us.

Photon-trapping is important at any radius where the accretion time scale is longer than the photon diffusion time scale from the disk midplane to the surface (Begelman 1978). The photons produced in this region of the disk are advected into the central BH and are unable to escape from the flow. Begelman considered only spherically symmetric accretion, but it is recognized that photon-trapping is important even for systems with a disk geometry.

Photon-trapping has been included approximately in the so-called “slim disk model” proposed by Abramowicz, Igumenshchev & Lasota (1998), and in recent calculations by Szuszkiewicz et al. (1996), Watarai et al. (2000), as well as in numerical simulations by Honma et al. (1991), Szuszkiewicz & Miller (1997), and Watarai & Mineshige (2003). However, these studies do not include the effect fully since they consider vertically integrated quantities in the disk and reduce the problem to a one-dimensional model. Full two-dimensional radiation-hydrodynamical simulations (2D-RHD) that include multi-dimensional effects were done for the first time by one of the current authors in Ohsuga et al. (2005)³.

* E-mail: k.kohri@lancaster.ac.uk

¹ We note that Ichimaru (1977) proposed similar ideas 20 years earlier.

² For recent developments on the RIAF model of Sgr. A*, see Manmoto, Kusunose & Mineshige. (1997), Yuan, Cui & Narayan (1995) and references therein.

³ Eggum et al. (1988) performed the first 2D numerical simulations of supercritical accretion disks, and their work was later improved by Okuda (2002). However, the computation time in

As we explain later, two multi-dimensional effects are important: i) Even at disk radii inside the trapping radius, photons that are emitted near the surface of the disk can escape, though most of the photons emitted deeper inside are advected into the BH. ii) The vertical profiles of various quantities in the disk such as density, optical depth, etc., play a critical role in determining what fraction of the photons escape, and thereby influence the total luminosity of the disk.

The first effect was pointed out and studied by Ohsuga et al. (2002) using simple analytical models and numerical simulations. In this paper, we include the second effect and study the combined influence of both effects for a broad class of accretion-disk models. We develop an analytical model of multi-dimensional effects and show that it agrees well with the numerical results of Ohsuga et al. (2005).

The results obtained here may change the current understanding of models such as the slim-disk and convection-dominated accretion flow (CDAF, Stone, Pringle & Begelman 1999; Narayan, Igumenshchev & Abramowicz 2000; Quataert & Gruzinov 2000; Igumenshchev, Abramowicz & Narayan 2000) models, as well as the neutrino-dominated accretion flow (NDAF) model (Popham, Woosley & Fryer. 1999; Narayan, Piran & Kumar 2001; Kohri & Mineshige 2002; Di Matteo, Perna & Narayan 2002; Kohri, Narayan & Piran 2005 Gu, Liu & Lu, 2006) which is believed to play an important role in the central engine of GRBs (Narayan, Paczynski & Piran 1992).⁴

We use z to represent the vertical direction with respect to the equatorial plane of the disk. We also assume that the temperature T in the disk is lower than the electron mass ($kT < m_e c^2$), so that the electrons are nonrelativistic.

2 STANDARD ONE-DIMENSIONAL APPROXIMATIONS

In this section we introduce the standard one-dimensional (1D) treatment of accretion disks, following the approach described in Ohsuga et al (2002). In this approach, we integrate along the z -axis and omit the z -dependences of the various astrophysical quantities. For instance, we write the optical depth from the mid-plane of the disk ($z = 0$) to the surface ($z = z_{\max}$) as

$$\tau = \int_0^{z_{\max}} dz \sigma_{\gamma e} n_e \quad (1)$$

$$\simeq \sigma_{\text{T}} n_e H, \quad (2)$$

where $\sigma_{\gamma e}$ is the scattering cross section of a photon off an electron. Although $\sigma_{\gamma e}$ depends in general on the photon energy E_γ , we limit ourselves to Thomson scattering, for which the cross-section is independent of energy. This is reasonable for the low energy photons $E_\gamma \ll \mathcal{O}(\text{MeV})$ of interest to us.

these studies was short and the numerical models did not reach steady state. Ohsuga et al. (2005) were the first to successfully compute models approaching steady state.

⁴ The relativistic magnetohydrodynamic (MHD) jet model is another attractive model of energetic accretion sources (e.g., McKinney 2005; 2006 and references therein). This model is less likely to be affected by our work.

H is the disk half-thickness and n_e is the electron number density in the disk mid-plane.

The diffusion time scale for a photon to escape from the disk mid-plane is given by

$$t_{\text{diff}} \approx N_{\text{scatt}} \lambda/c, \quad (3)$$

where N_{scatt} is the number of scatterings, $\lambda = 1/(\sigma_{\text{T}} n_e)$ is the mean free path, and c is the speed of light. Since N_{scatt} is given by

$$N_{\text{scatt}} \approx 3 \tau^2, \quad (4)$$

(assuming a random walk in three-dimensions, see Appendix B), we write

$$t_{\text{diff}} \approx 3\tau H/c. \quad (5)$$

The accretion time scale is

$$t_{\text{acc}} = -\frac{R}{v_r}, \quad (6)$$

where the radial velocity v_r is related to the mass accretion rate \dot{M} and the density ρ by

$$v_r = -\frac{\dot{M}}{4\pi R \int_0^H \rho dz} \quad (7)$$

$$= -\frac{\dot{M}}{4\pi R \rho H}. \quad (8)$$

Thus

$$t_{\text{acc}} \approx \frac{\tau}{\dot{m}} \frac{R^2}{c R_g}, \quad (9)$$

where we have set $\rho \approx m_p n_e$ and introduced a dimensionless mass accretion rate \dot{m} ,

$$\dot{m} = \dot{M}/\dot{M}_{\text{crit}}. \quad (10)$$

The critical mass accretion rate \dot{M}_{crit} is defined in terms of the Eddington luminosity L_E as follows, $\dot{M}_{\text{crit}} = L_E/c^2$, where $L_E = 4\pi c G m_p M/\sigma_{\text{T}} \simeq 1.3 \times 10^{38} \text{erg sec}^{-1} (M/M_\odot)$ for a black hole of mass M .

Photons can escape from the disk only if the condition $t_{\text{diff}} < t_{\text{acc}}$ is satisfied. Therefore, the disk radiates freely only from radii larger than a certain limit,

$$R > R_{\text{trap}}, \quad (11)$$

where the trapping radius R_{trap} is given by

$$R_{\text{trap}} = \frac{3}{2} h_{\text{in}} \dot{m} R_g. \quad (12)$$

Here $R_g = 2GM/c^2$ is the Schwarzschild radius, and

$$h_{\text{in}} \equiv \left. \frac{H}{R} \right|_{R \leq R_{\text{trap}}}, \quad (13)$$

assuming that, when $R < R_{\text{trap}}$ and radiation is trapped, the disk is geometrically thick with $h_{\text{in}} \sim 1$ and that h here is independent of R . As we show in Appendix A, h is indeed constant (≈ 0.5) for $R \leq R_{\text{trap}}$ and decreases $\propto 1/R$ for $R_{\text{trap}} < R$. This validates Eq. (12). Note that R_{trap} is proportional to \dot{m} .

The energy released in the disk per unit time by viscous dissipation is given by

$$L = 2 \int_{R_{\text{in}}}^{R_{\text{out}}} 2\pi R Q_{\text{vis}}(R) dR, \quad (14)$$

where the viscous heating rate is

$$Q_{\text{vis}}(R) = \frac{3}{8\pi} \frac{GM}{R^3} \dot{M} \left[1 - \left(\frac{R_{\text{in}}}{R} \right)^{1/2} \right]. \quad (15)$$

Here R_{in} and R_{out} are the radii of the inner and outer edge of the disk. However, not all the released energy is radiated because of photon-trapping. We discuss two cases below, depending on whether R_{trap} is larger or smaller than R_{in} . For readers' convenience we introduce a dimensionless inner radius normalized by the Schwarzschild radius.

$$r_{\text{in}} \equiv R_{\text{in}}/R_g. \quad (16)$$

2.1 $R_{\text{trap}} < R_{\text{in}}$

When $R_{\text{trap}} < R_{\text{in}}$, there is no trapped region and we estimate the total luminosity to be

$$\begin{aligned} L_{1\text{D,tot},R_{\text{trap}} < R_{\text{in}}} &= 2 \int_{R_{\text{in}}}^{\infty} 2\pi R Q_{\text{vis}}(R) dR \\ &= \frac{1}{6h_{\text{in}}} L_E \frac{R_{\text{trap}}}{R_{\text{in}}} \\ &= \frac{L_E}{4r_{\text{in}}} \dot{m}, \end{aligned} \quad (17)$$

which is linearly proportional to \dot{m} . This is a well known result for the standard thin accretion disk model in Newtonian gravity.

2.2 $R_{\text{in}} < R_{\text{trap}}$

When $R_{\text{in}} < R_{\text{trap}}$, only the region of the disk outside R_{trap} radiates freely and the luminosity from this region of the disk is

$$\begin{aligned} L_{1\text{D},R_{\text{trap}} < R} &= 2 \int_{R_{\text{trap}}}^{\infty} 2\pi R Q_{\text{vis}}(R) dR \\ &= \frac{1}{2h_{\text{in}}} L_E \left[1 - \frac{2}{3} \left(\frac{R_{\text{trap}}}{R_{\text{in}}} \right)^{-1/2} \right] \\ &= \frac{1}{2h_{\text{in}}} L_E \left[1 - \sqrt{\frac{8r_{\text{in}}}{27h_{\text{in}}}} \dot{m}^{-1/2} \right]. \end{aligned} \quad (18)$$

Within the one-dimensional approximation being discussed in this section, it is unclear how much luminosity is emitted from the region of the disk $R_{\text{in}} < R < R_{\text{trap}}$. One extreme assumption is that there is no luminosity at all from this region, as in Ohsuga et al. 2002. Alternatively, one might assume that the disk flux here is limited to the local Eddington flux $F \approx F_E(R) = L_E/(4\pi R^2) = GMm_p c/(R^2 \sigma_T)$. The luminosity from $R_{\text{in}} < R < R_{\text{trap}}$ of the disk is then given by

$$\begin{aligned} L_{1\text{D},R < R_{\text{trap}}} &= 2 \int_{R_{\text{in}}}^{R_{\text{trap}}} 2\pi R F_{\text{Edd}}(R) dR \\ &= L_E \ln \left(\frac{R_{\text{trap}}}{R_{\text{in}}} \right) \\ &= L_E \ln \left(\frac{3h_{\text{in}}}{2r_{\text{in}}} \dot{m} \right). \end{aligned} \quad (19)$$

If we include the term given in Eq. (18), keeping in mind that it is uncertain, then the ‘‘total luminosity’’ becomes

$$L_{1\text{D,tot},R_{\text{in}} < R_{\text{trap}}}$$

$$\begin{aligned} &= L_{1\text{D},R_{\text{trap}} < R} + L_{1\text{D},R < R_{\text{trap}}} \\ &= \frac{1}{2h_{\text{in}}} L_E \left[1 + 2h_{\text{in}} \ln \left(\frac{R_{\text{trap}}}{R_{\text{in}}} \right) - \frac{2}{3} \left(\frac{R_{\text{trap}}}{R_{\text{in}}} \right)^{-1/2} \right] \\ &= \frac{1}{2h_{\text{in}}} L_E \left[1 + 2h_{\text{in}} \ln \left(\frac{3h_{\text{in}}}{2r_{\text{in}}} \dot{m} \right) - \sqrt{\frac{8r_{\text{in}}}{27h_{\text{in}}}} \dot{m}^{-1/2} \right]. \end{aligned} \quad (20)$$

Note that the luminosity is reduced relative to the result in Eq. (17) for the untrapped case, and increases only logarithmically with \dot{m} . This explains why disks with supercritical accretion ($\dot{m} \gg 1$, ‘‘slim’’ disks) are radiatively inefficient.

3 TWO-DIMENSIONAL EFFECTS

So far we have discussed a 1D approximation and assumed somewhat arbitrarily that the region $R < R_{\text{trap}}$ either does not radiate at all or radiates at the local Eddington rate. In this section we carry out a more careful two-dimensional analysis. We focus on the region $R_{\text{in}} \leq R < R_{\text{trap}}$ discussed in Subsection 2.2, but now we carefully consider the two-dimensional distribution of quantities.

In the following, we consider most of the quantities in the disk to depend on both R and z (the vertical height). However, we assume that the thin-disk approximation is approximately valid in the sense that we omit the z -dependence when considering hydrostatic balance in the z -direction ($c_S = \Omega_K H$, with the sound speed c_S and the Keplerian angular velocity $\Omega_K = \sqrt{GM/R^3}$) and angular momentum conservation ($\nu \int \rho dz = \dot{M}(1 - \sqrt{R_{\text{in}}/R})/(3\pi)$, with the kinetic viscosity ν). Then the z -dependent optical depth at a given R is given by

$$\tau(z) = \int_z^{z_{\text{max}}} dz \sigma_{\gamma e} n_e(z) \quad (21)$$

$$\simeq \sigma_T \int_z^{z_{\text{max}}} dz n_e(z), \quad (22)$$

where $n_e(z)$ is the electron number density at height z , and z_{max} corresponds to the upper surface of the disk. We see that the expression for τ given in Eq. (1) in the 1D approximation corresponds to $\tau(0)$ in Eq. (21).

We now introduce a detailed model for the vertical electron density profile. As seen in Fig. 1, we can fit the the density profile found in the numerical simulation in Ohsuga et al. (2005) quite well with the following power-law form,

$$n_e(z) = n_e(0) \left(1 - \frac{z}{qH} \right)^{q-1} \quad (q \geq 1, \text{ and } 0 \leq z \leq qH), \quad (23)$$

where $n_e(0)$ and the power-law index q may depend on the radius R . In the limit as $q \rightarrow \infty$, this model takes the form of an exponential ⁵

$$n_e(z) = n_e(0) \exp \left(-\frac{z}{H} \right) \quad (0 \leq z \leq \infty), \quad (24)$$

⁵ If on the other hand we have a constant z -independent density, as considered by Ohsuga et al. (2002), it would correspond to $q = 1$. The corresponding results can be recovered by setting $q = 1$ in all the expressions in the current paper.

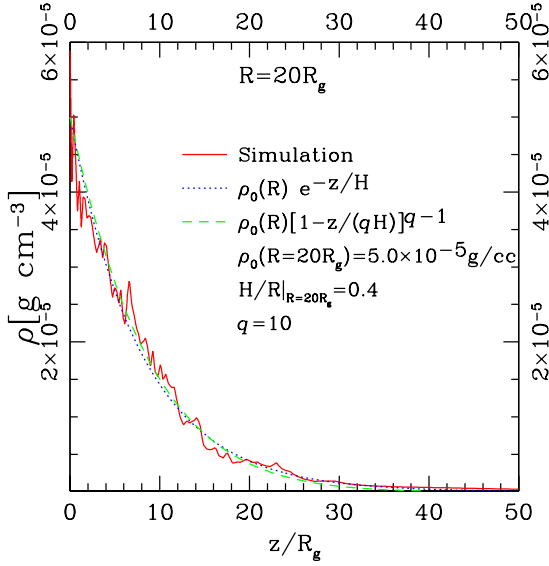


Figure 1. Matter density profile along with the z -axis for a fixed R . Here we show a case of $R = 20R_g$. The solid line represents the result in the numerical simulation in Ohsuga et al. (2002). We can fit the data well by assuming that the profile has the exponential or the power-law shape. The dotted (dashed) line represents the exponential (power-law) profile. Here we took $H/R = 0.4$ and $q = 10$. We have also checked that generally we can fit the numerical results in Ohsuga et al. (2002) by the above functional forms by adopting $H/R = 0.4$ for all ranges of R up to $\sim 50R_g$.

The optical depth from z to the surface is

$$\tau(z) = \tau(0) \left(1 - \frac{z}{qH}\right)^q, \quad (25)$$

except for $q \rightarrow \infty$ when it takes an exponential form.

Because we adopt the numerical results corresponding to $\dot{m} \gtrsim 100$ in Ohsuga et al. (2005), the radii R of order tens of R_g that we consider are smaller than $R_{\text{trap}} \sim 10^2 R_g$ and so we are in the radiation-trapped regime. Note that Fig. 1 gives $H/R \approx 0.4$ for the numerical simulation of Ohsuga et al. (2005), which is approximately consistent with the approximation $h_{\text{in}} = 0.5$ that we made in the previous section and in Appendix A.

The photon diffusion time scale from height z to the surface of the disk at z_{max} is given by

$$t_{\text{diff}}(z) \approx N_{\text{scatt}}(z, z_{\text{max}}) \lambda(z)/c, \quad (26)$$

where $N_{\text{scatt}}(z, z_{\text{max}})$ is the number of scatterings in the 3D random walk,

$$N_{\text{scatt}}(z, z_{\text{max}}) = 3 [\tau(z)]^2, \quad (27)$$

and $\lambda(z)$ is the mean free path which is estimated using the properties of the disk at the starting position z of the photon

$$\lambda(z) = \frac{1}{\sigma_{\text{T}} n_e(z)}. \quad (28)$$

The detailed derivation of the above relation is given in Appendix B. By using Eqs. (27) and (28), we obtain an expression for the z -dependent diffusion time scale,

$$\begin{aligned} t_{\text{diff}}(z) &= 3\tau(z)^2 \lambda(z)/c \\ &= 3\tau(0) \frac{H}{c} \left[\frac{\tau(z)}{\tau(0)} \right]^{(q+1)/q}. \end{aligned} \quad (29)$$

By requiring the diffusion time scale $t_{\text{diff}}(z)$ to be shorter than the accretion time scale t_{acc} given in Eq. (9), we find that photons can escape only from the region where the following condition is satisfied,

$$\frac{\tau(z)}{\tau(0)} < \left(\frac{R}{R_{\text{trap}}} \right)^{q/(q+1)}, \quad (30)$$

The photon-trapping radius R_{trap} is determined by Eq. (12) and is proportional to \dot{m} . A schematic picture indicating the region of the disk from which radiation can escape is shown in Fig. 2. We see that trapping is not determined by simply a critical radius R_{trap} , but is described in terms of a two-dimensional surface $z_{\text{trap}}(R)$, where

$$\frac{\tau(z_{\text{trap}})}{\tau(0)} \equiv \left(\frac{R}{R_{\text{trap}}} \right)^{q/(q+1)}. \quad (31)$$

Note that z_{trap} is a function of R in this case given by

$$z_{\text{trap}} = qH \left[1 - \left(\frac{R}{R_{\text{trap}}} \right)^{1/(q+1)} \right], \quad (32)$$

and its derivative by R is always negative $dz_{\text{trap}}/dR < 0$ because

$$\frac{dz_{\text{trap}}}{dR} = -\frac{q}{q+1} \frac{H}{R_{\text{trap}}} \left(\frac{R}{R_{\text{trap}}} \right)^{-q/(q+1)}. \quad (33)$$

The luminosity from the region $R_{\text{in}} \leq R \leq R_{\text{trap}}$ is then given by

$$L_{2\text{D}, R < R_{\text{trap}}} = 2 \int_{R_{\text{in}}}^{R_{\text{trap}}} 2\pi R Q_{\text{vis}}(R) \frac{\tau(z_{\text{trap}})}{\tau(0)} dR. \quad (34)$$

Here we assume that all the energy released at $z \geq z_{\text{trap}}$ is radiated, while the energy released at $z < z_{\text{trap}}$ is completely trapped. Also, because Q_{vis} and $\tau(z)$ are both proportional to $\int \rho dz$, we express the vertical distribution of viscous dissipation directly by means of the factor $\tau(z_{\text{trap}})/\tau(0)$.

Evaluating the above integral, we obtain the luminosity of the disk from the region $R < R_{\text{trap}}$:

$$\begin{aligned} L_{2\text{D}, R < R_{\text{trap}}} &= 2 \int_{R_{\text{in}}}^{R_{\text{trap}}} 2\pi R Q_{\text{vis}}(R) \left(\frac{R}{R_{\text{trap}}} \right)^{q/(q+1)} dR \\ &= \frac{1}{2h_{\text{in}}} L_{\text{E}} \left(\frac{R_{\text{trap}}}{R_{\text{in}}} \right)^{1/(q+1)} \\ &\quad \times \int_1^{R_{\text{trap}}/R_{\text{in}}} dx \frac{1}{x^{(q+2)/(q+1)}} \left(1 - \frac{1}{x^{1/2}} \right) \\ &= \frac{1}{2h_{\text{in}}} L_{\text{E}} \times \\ &\quad \left[\frac{2(q+1)}{q+3} \left(\frac{R_{\text{trap}}}{R_{\text{in}}} \right)^{-1/2} + \frac{(q+1)^2}{q+3} \left(\frac{R_{\text{trap}}}{R_{\text{in}}} \right)^{1/(q+1)} - (q+1) \right] \\ &= \frac{1}{2h_{\text{in}}} L_{\text{E}} \times \end{aligned} \quad (35)$$

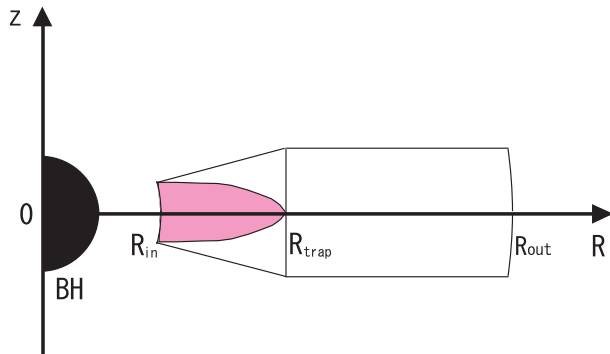


Figure 2. Schematic picture of the disk around a BH. Even if $R < R_{\text{trap}}$, there surely exists a region from which the diffusion of photons occurs (white region). The shaded region represents the “actual” photon-trapping region from which any photons can never escape in the flow.

$$\left[\frac{2(q+1)}{q+3} \left(\frac{3h_{\text{in}}\dot{m}}{2r_{\text{in}}} \right)^{-1/2} + \frac{(q+1)^2}{q+3} \left(\frac{3h_{\text{in}}\dot{m}}{2r_{\text{in}}} \right)^{1/(q+1)} - (q+1) \right].$$

The dominant contribution comes from the second term, which is proportional to $\dot{m}^{1/(q+1)}$ for $\dot{m} \gg 1$. The luminosity from the region $R_{\text{trap}} < R$ is, of course, the same as in the 1D case (Eq. 18), i.e., $L_{2\text{D}, R_{\text{trap}} < R} = L_{1\text{D}, R_{\text{trap}} < R}$, since there is no photon trapping. Therefore, we have the following expression for the total radiated luminosity from the entire disk,

$$\begin{aligned} L_{2\text{D}, \text{tot}}(q) &= L_{2\text{D}, R < R_{\text{trap}}} + L_{2\text{D}, R_{\text{trap}} < R} \\ &= \frac{1}{2h_{\text{in}}} L_{\text{E}} \times \\ &\left[\frac{4q}{3(q+3)} \left(\frac{R_{\text{trap}}}{R_{\text{in}}} \right)^{-1/2} + \frac{(q+1)^2}{q+3} \left(\frac{R_{\text{trap}}}{R_{\text{in}}} \right)^{1/(q+1)} - q \right] \\ &= \frac{1}{2h_{\text{in}}} L_{\text{E}} \times \quad (36) \\ &\left[\frac{4q}{3(q+3)} \left(\frac{3h_{\text{in}}\dot{m}}{2r_{\text{in}}} \right)^{-1/2} + \frac{(q+1)^2}{q+3} \left(\frac{3h_{\text{in}}\dot{m}}{2r_{\text{in}}} \right)^{1/(q+1)} - q \right]. \end{aligned}$$

In a similar fashion, we obtain the following result for the case of an exponential density profile ($q \rightarrow \infty$),

$$\begin{aligned} L_{2\text{D}, \text{tot}}(q = \infty) &= \frac{1}{2h_{\text{in}}} L_{\text{E}} \left[\frac{4}{3} \left(\frac{R_{\text{trap}}}{R_{\text{in}}} \right)^{-1/2} + \ln \left(\frac{R_{\text{trap}}}{R_{\text{in}}} \right) - 1 \right] \quad (37) \\ &= \frac{1}{2h_{\text{in}}} L_{\text{E}} \left[\sqrt{\frac{32r_{\text{in}}}{27h_{\text{in}}}} \dot{m}^{-1/2} + \ln \left(\frac{3h_{\text{in}}\dot{m}}{2r_{\text{in}}} \right) - 1 \right]. \end{aligned}$$

To verify that this result is consistent with the limit $q \rightarrow \infty$ of Eq. (35), we make use of the following useful relation,

$$\lim_{\varepsilon \rightarrow 0} \frac{1}{\varepsilon} \left[\frac{1}{2\varepsilon + 1} x^\varepsilon - 1 \right] = \ln x - 2. \quad (38)$$

This shows that the dominant terms in Eq. (35) do not diverge as $q \rightarrow \infty$ but tend to a finite value that is proportional to $\ln(\dot{m})$ for $\dot{m} \gg 1$.

4 COMPARISON WITH NUMERICAL SIMULATION

Here we compare the analytical formulae derived above for the luminosity L of the disk with the results of multi-dimensional numerical simulations reported by Ohsuga et al. (2005).

In Fig. 3 we plot the disk luminosity in Eddington units as a function of the dimensionless mass-accretion rate \dot{m} . Analytical formulae are denoted by solid lines and correspond, in descending order, to the following cases: no photon-trapping (Eq. 17), power-law density profile with $q = 1$ and $q = 10$ (Eq. 36), exponential density profile (Eq. 37, i.e., $q \rightarrow \infty$), and the standard 1D model which ignores photons emitted from $R_{\text{in}} < R < R_{\text{trap}}$ (Eq. 19). Triangles, circles, and squares connected by long-dashed lines indicate the numerical results from Fig. 7 of Ohsuga et al. (2005) corresponding to metallicity $Z = 0, 1Z_{\odot}$, and $10Z_{\odot}$, respectively. For details see Ohsuga et al. (2005). The dotted line represents the results of the hydrodynamical simulations of the slim-disk model carried out by Watarai et al. (2000), which did not explicitly include two-dimensional effects. Here we adopted $R_{\text{in}} = 3R_{\text{g}}$ and $h = 0.4$.

From Fig. 3 we see that the luminosity is larger than with the standard analytical 1D model if we ignore radiation from the photon-trapped region. The increase is the result of the multi-dimensional effects which allow photons to diffuse and partially escape even from radii $R < R_{\text{trap}}$.

For reference, we have also plotted by a short-dashed line the approximate formula Eq. (20) for the disk luminosity in the 1D model, which includes the photon luminosity emitted from $R_{\text{in}} < R < R_{\text{trap}}$ by assuming a simple local Eddington flux. Because of the logarithmic functional form of this approximation, this model resembles the exponential density model in the 2D treatment. Correspondingly, we conclude that this model provides a reasonable way of approximating multi-dimensional effects within the 1D approach.

Ohsuga et al. (2005) pointed out that photons tend to have momenta pointed inwards because of advection by the accretion flow, which causes the radiation to spend a longer time in the disk before escaping relative to the simple diffusion estimate we have used in our model. However, we believe this introduces only a minor correction to our results because we are focusing mainly on photons for which $t_{\text{diff}} < t_{\text{acc}}$.

In addition, Ohsuga et al. (2002) obtained outflows driven by the super Eddington luminosity of their models. Although our analytical model does not include outflows, we believe our discussion is still applicable in a time-averaged mean sense.

5 DISCUSSION AND CONCLUSION

In this paper, we have studied multi-dimensional effects on the luminosity emitted from an accretion disk. In the usual one-dimensional treatment of disks, one integrates all quantities along the vertical (z) direction. This is reasonable for a thin accretion disk when the accretion rate is well below the Eddington rate. However, we show that, when the accretion rate is large, it is quite important to consider the z -dependence of fluid quantities and treat the vertical diffusion

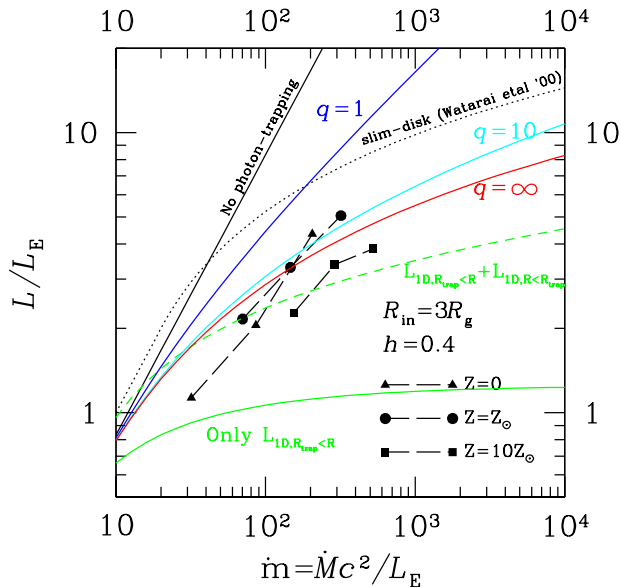


Figure 3. Luminosity as a function of the mass-accretion rates. Analytical formulae are denoted by solid lines. They are the cases of the no photon-trapped regions, the power-law cases with $q = 1$, and $q = 10$, the exponential case which corresponds to $q = \infty$, and the standard analytical 1D model ignoring any photons emitted from $R_{\text{in}} < R < R_{\text{trap}}$, in descending order. The symbols of triangles, circles, and squares connected by long-dashed lines indicate the numerical results in Fig. 7 in Ohsuga et al. (2005), in case of the metallicity $Z = 0$, Z_{\odot} , and $10 Z_{\odot}$, respectively. The dotted line represents the case of the hydrodynamical simulations of slim-disk in Watarai et al. (2001), without explicitly including 2D effects. We also plot the speculated total luminosity calculated in the analytical 1D model (short-dashed line), which includes the photon luminosity emitted from $R_{\text{in}} < R < R_{\text{trap}}$ by assuming a simple local Eddington flux. Here we adopted $R_{\text{in}} = 3R_g$ and $h = 0.4$.

of photons carefully. If we omit the z -dependence on the diffusion process in the simplest version of the one-dimensional model, we tend to significantly underestimate the luminosity. On the other hand, if we omit the z -dependences of the matter density and assume uniform density, we overestimate the luminosity. Only when we consider the z -dependence on the matter density and adopt the appropriate density profile such as a power-law or exponential form as a function of z , as seen in 2D radiation-hydrodynamical simulations, are we able to reproduce the luminosity found in the numerical simulations.

Using the analytical approach developed here, we should be able to model how the peak energy of the photon spectrum decreases when the photons produced near the BH are trapped, as pointed out by Ohsuga et al. (2003). This will be discussed in a forthcoming paper (Kohri & Ohsuga, 2007).

When we simultaneously include radiative, advective, convective, and neutrino cooling processes in an analytical

model of the accretion disk, multi-dimensional effects will play a crucial role. In neutrino dominated accretion flows (NDAFs), for instance, the neutrino luminosity and annihilation rate could be modified substantially relative to the predictions of one-dimensional models. The dominant cooling process could thus be changed by multi-dimensional effects, and the entire picture of the accretion might be dramatically modified, e.g., for the produced energy through the $\nu \bar{\nu}$ annihilation (Di Matteo, Perna & Narayan 2002, Gu, Liu & Lu 2006, Chen & Beloborodov), r -process nucleosynthesis (Surman, McLaughlin, Hix 2006), and so on. We plan to discuss these effects in forthcoming papers.

Multi-dimensional hydrodynamic simulations of accretion disks including all of these cooling processes have not been done so far (except for the 2D numerical simulations of neutrino cooled disks by Lee & Ramirez-Ruiz, 2006). To clarify the role of multi-dimensional effects on CDAFs, NDAFs, etc., it would be useful to compare the analytical estimates with full multi-dimensional numerical simulations. It is hoped that these simulations will be done in the near future.

ACKNOWLEDGEMENTS

K.K. would like to thank A. E. Broderick, J. C. McKinney and S. Mineshige for valuable discussions at an early stage of this work. This work was supported in part by NASA grant NNG04GL38G, PPARC grant, PP/D000394/1, EU grant MRTN-CT-2006-035863, the European Union through the Marie Curie Research and Training Network "UniverseNet" (MRTN-CT-2006-035863), and Research Grant from Japan Society for the Promotion of Science (17740111).

APPENDIX A: ANALYTICAL ESTIMATES OF DISK-HALF THICKNESS H

In this section, we simply try to analytically estimate the R -dependence on disk-half thickness H . The force balance along z -axis is generally expressed by

$$\frac{\sigma_T}{m_p c} F = \frac{GM}{R^2} \frac{H}{R}, \quad (\text{A1})$$

with a photon flux of F .

If $R_{\text{trap}} < R$, then it would be reasonable to assume that the flux is equal to the viscous heating rate, $F \approx Q_{\text{vis}}$. Then, we obtain

$$\left. \frac{H}{R} \right|_{R_{\text{trap}} < R} \approx \frac{3}{4} \frac{R_g}{R} \dot{m}. \quad (\text{A2})$$

Therefore H/R is approximately proportional to $\propto 1/R$ for $R_{\text{trap}} < R$.

On the other hand, if $R < R_{\text{trap}}$, we may assume that the flux would be approximately the order of the Eddington flux $F \approx \frac{1}{2} F_E = \frac{1}{2} L_E / (4\pi R^2)$. The factor 1/2 in front of F_E is attached as a matter of convenience for the consistency. That comes from the viewpoint of continuities of astrophysical quantities although physics does not change at all by this artificial factor. From Eq. (A1) we find that H/R is constant for $R < R_{\text{trap}}$,

$$\left. \frac{H}{R} \right|_{R < R_{\text{trap}}} \approx \frac{1}{2}. \quad (\text{A3})$$

Then we see that $h = H/R$ is a smooth function as R ,

$$h = \begin{cases} 1/2 & (R \leq R_{\text{trap}}), \\ \frac{1}{2}R_{\text{trap}}/R & (R_{\text{trap}} < R), \end{cases} \quad (\text{A4})$$

if we take $R_{\text{trap}} = 3/2h_{\text{in}}\dot{m}R_g$ with $h_{\text{in}} = 1/2$.

APPENDIX B: DERIVATION OF THE Z-DEPENDENT/INDEPENDENT DIFFUSION TIME SCALE

Here we discuss the diffusion time scale along with z -axis in 3D random walk processes when the scattering length depends on the position, i.e., in the case that we consider the z -dependent number density of electron, the cross section, and so on in the electron-photon scattering processes.

In general, we can write the summed distance measured along the 3D random walk process from the starting point $z = z_0$ as

$$d(z_0, z_{\text{max}}) = \sum_{i_z=1}^{N_{\text{scatt}}(z_0, z_{\text{max}})} \int_{z_{i_z-1}}^{z_{i_z}} dz, \quad (\text{B1})$$

where $N_{\text{scatt}}(z_0, z_{\text{max}})$ is the number of the scattering from $z = z_0$ to a maximum of z ($\equiv z_{\text{max}}$). The integral interval $[z_{i_z-1}, z_{i_z}]$ is determined by solving the following differential equation for the number of the scattering,

$$\frac{dN}{dz} = \sigma_{\gamma e} n_e(z). \quad (\text{B2})$$

When we solve it, we may assume that the interval between the scatterings is determined by the approximate relation,

$$\left| \int_{z_{i_z-1}}^{z_{i_z}} \sigma_{\gamma e} n_e(z) dz \right| = \frac{1}{3}, \quad (\text{B3})$$

where the meaning of dividing by three comes from the contribution only to z -axis in the the 3D random walk. Of course the right hand side would not have to be one third if only it were the order of $\mathcal{O}(1)$. For simplicity, here we have just took it one third. In addition, generally z_{i_z} must not be larger than z_{i_z-1} .

As we will see later, the diffusion tends to be proceeded outward with increasing the diffusion length or the mean free path. Then the time spent in inner regions tends to be much longer than that in outer ones. That means that phenomena of the diffusion which started from $z = z_0$ are mainly determined by the local physics at around $z = z_0$. Then Eq. (B3) might be rewritten as a definition of the z -dependent mean-free path $\lambda(z)$ through

$$\int_{z_{i_z-1}}^{z_{i_z}} \sigma_{\gamma e} n_e(z) dz \approx \sigma_{\text{T}} n_e(z_{i_z-1}) \int_{z_{i_z-1}}^{z_{i_z}} dz, \quad (\text{B4})$$

by

$$\lambda(z_{i_z-1}) \equiv \left| \int_{z_{i_z-1}}^{z_{i_z}} dz \right| \approx \frac{1}{3} \frac{1}{\sigma_{\text{T}} n_e(z_{i_z-1})}, \quad (\text{B5})$$

where we assumed that $\sigma_{\gamma e} = \sigma_{\text{T}}$. Although there would be a lot of ways to define the z -dependent mean-free path, the definition in Eq. (B5) would be relatively natural in the current context of the accretion disks because the phenomena are mainly locally determined.

Then $d(z_0, z_{\text{max}})$ in Eq. (B1) is rewritten as

$$d(z_0, z_{\text{max}}) = \sum_{i_z=1}^{N_{\text{scatt}}(z_0, z_{\text{max}})} \ell(z_{i_z-1}), \quad (\text{B6})$$

with

$$\ell(z_{i_z}) = \begin{cases} \lambda(z_{i_z}) & (z_{i_z+1} \geq z_{i_z}), \\ -\lambda(z_{i_z}) & (z_{i_z+1} < z_{i_z}). \end{cases} \quad (\text{B7})$$

Next let us consider the averaged value of $d(z)$ after sufficiently a lot of tries.

$$\langle d(z_0, z_{\text{max}}) \rangle = \sum_{i_z=1}^{N_{\text{scatt}}(z_0, z_{\text{max}})} \langle \ell(z_{i_z-1}) \rangle, \quad (\text{B8})$$

where $\langle X \rangle$ means the average of X after such trials. Here we can assume $\langle \ell(z_{i_z-1}) \rangle \approx 0$. That is because we have assumed that the local physics at around $z = z_{i_z-1}$ determines the phenomena, and surely then this approximation would not be so bad. Then we see that the averaged value of $d(z_0, z_{\text{max}})$ vanishes,

$$\langle d(z_0, z_{\text{max}}) \rangle \approx 0. \quad (\text{B9})$$

On the other hand, however, the averaged value of the square of $d(z)$ must be finite.

$$\begin{aligned} \langle d(z_0, z_{\text{max}})^2 \rangle &= \sum_{i_z=1}^{N_{\text{scatt}}(z_0, z_{\text{max}})} \sum_{j_z=1}^{N_{\text{scatt}}(z_0, z_{\text{max}})} \langle \ell(z_{i_z-1}) \ell(z_{j_z-1}) \rangle \\ &= \sum_{i_z=j_z=1}^{N_{\text{scatt}}(z_0, z_{\text{max}})} \langle \ell(z_{i_z-1})^2 \rangle + \sum_{i_z \neq j_z} \langle \ell(z_{i_z-1}) \ell(z_{j_z-1}) \rangle \\ &\approx \sum_{i_z=j_z=1}^{N_{\text{scatt}}(z_0, z_{\text{max}})} \langle \lambda(z_{i_z-1})^2 \rangle, \end{aligned} \quad (\text{B10})$$

where we approximated

$$\begin{aligned} \sum_{i_z \neq j_z} \langle \ell(z_{i_z-1}) \ell(z_{j_z-1}) \rangle &\approx \sum_{i_z \neq j_z} \ell(z_{i_z-1}) \langle \ell(z_{j_z-1}) \rangle \left(\approx \sum_{i_z \neq j_z} \langle \ell(z_{i_z-1}) \ell(z_{j_z-1}) \rangle \right) \\ &\approx 0, \end{aligned} \quad (\text{B11})$$

because the step i_z does not correlate with that of j_z among the independent trials for $\langle \ell(z_{i_z-1}) \rangle = 0$. Now we can approximate $\langle \lambda(z_{i_z-1})^2 \rangle \approx \lambda(z_0)^2$ because the scatterings at the outer regions do not frequently occur and hardly contribute to the summation at all.

Then from (B10), we find that the number of the scattering of the photon diffused from z to z_{max} , i.e., $\langle d^2(z, z_{\text{max}}) \rangle = (\int_z^{z_{\text{max}}} dz)^2$, is represented by⁶

$$\begin{aligned} N_{\text{scatt}}(z, z_{\text{max}}) &\approx 3 [\sigma_{\text{T}} n_e(z)]^2 \left(\int_z^{z_{\text{max}}} dz \right)^2 \\ &\approx 3 \left[\sigma_{\text{T}} \int_z^{z_{\text{max}}} dz n_e(z) \right]^2 \end{aligned}$$

⁶ Note that we have removed the subscript “0” in z .

$$= 3\tau(z)^2, \quad (\text{B12})$$

where we have used the same logic in Eq. (B4) to transform the first line to the second.

Here we get the expression of the z -dependent diffusion time scale,

$$\begin{aligned} t_{\text{diff}}(z) &\equiv N_{\text{scatt}}(z, z_{\text{max}})\lambda(z)/c \\ &\approx 3\tau(z)^2\lambda(z)/c. \end{aligned} \quad (\text{B13})$$

Of course, if we omit the z -dependence, we immediately get the z -independent diffusion time scale shown in Eqs. (3) and (5).

When we consider the power-law density profiles $\propto (1-z/qH)^{q-1}$ (or the exponential one as their large- q limit), surely $t_{\text{diff}}(z)$ decreases rapidly as $\propto (1-z/qH)^{q+1}$ as a function of z . This means that the time spent in the inner regions is much longer than that in the outer ones, that validates our assumption in the current context in the accretion disks.

REFERENCES

- Abramowicz, M.A., Chen X., Kato S. et al. 1995, ApJ 438, L37
 Abramowicz, M.A., Igumenshchev, I.V., Lasota, J.-P. 1998, MNRAS, 293, 443
 Begelman, M. C. 1978, MNRAS, 184, 53
 Di Matteo, T., Perna R., & Narayan, R., 2002, ApJ, 579, 706
 Chen, W.-X., & Beloborodov, A.M., astro-ph/0607145
 Eggum, G. E., Coroniti, F. V. & Katz, J. I. 1988, ApJ, 330, 142
 Gu, W.-M., Liu, T., & Lu, J.-F. 2006, ApJ, 643, L87
 Honma, F., Matsumoto, R., & Kato, S. 1991, PASJ, 43, 147
 Ichimaru, S. 1977, ApJ 214, 840
 Igumenshchev, I.V., Abramowicz, M.A., and Narayan, R., 2000, ApJ 537, L271
 Kohri, K., & Mineshige, S. 2002, ApJ, 577, 311,
 Kohri, K., Narayan, R., & Piran, T. 2005 ApJ, 629, 341
 Kohri, K., & Ohsuga, K. 2007, in preparation
 Lee, W. H. & Ramirez-Ruiz, E. 2006, ApJ, 641, L961
 Manmoto, T., Kusunowse M., Mineshige S. 1997, ApJ 489, 791
 McKinney, J. C. 2005, arXiv:astro-ph/0506367.
 McKinney, J. C. 2006, MNRAS, 368, 1561
 Narayan, R., Igumenshchev, I.V., and Abramowicz, M.A., 2000, ApJ 539, 798
 Narayan, R., Paczynski, B., & Piran, T., 1992, ApJ, 395L, 83
 Narayan, R., Piran, T., & Kumar, P. 2001, ApJ, 557, 949
 Ohsuga, K., Mineshige, S., Mori, M., & Umemura, M. 2002, ApJ, 574, 315
 Ohsuga, K., Mineshige, Watarai, K. 2003, ApJ, 596, 429
 Ohsuga, K., Mori, T. Nakamoto, M., & Mineshige, S. M. 2005, ApJ, 628, 368
 Okuda, T. 2002, PASJ, 54, 243
 Popham, R., Woosley, S.E., & Fryer, C., 1999, ApJ, 518, 356
 Quataert, E., & Gruzinov, A., 2000, ApJ 539, 809
 Surman, R., McLaughlin, G. C. & Hix, W. R., 2006, ApJ, 643, 1057

- Stone, J.M., & Pringle, J.E., 2000, MNRAS 322, 461
 Szuszkiewicz, E. et al., 1996, ApJ, 458, 474
 Szuszkiewicz, E. & Miller, J. C. 1997, MNRAS, 287, 165
 Watarai, K., Fukue, J., Takeuchi, M., & Mineshige, S. 2000, PASJ, 52, 133
 Watarai, K. & Mineshige, S. 2003, ApJ, 596, 421
 Yuan, F., Cui, W., & Narayan, R. 2005, ApJ, 620, 905